

Methodology for seismic risk assessment for tubular steel wind turbine towers: application to Canadian seismic environment

Elena Nuta, Constantin Christopoulos, and Jeffrey A. Packer

Abstract: The seismic response of tubular steel wind turbine towers is of significant concern as they are increasingly being installed in seismic areas and design codes do not clearly address this aspect of design. The seismic hazard is hence assessed for the Canadian seismic environment using implicit finite element analysis and incremental dynamic analysis of a 1.65 MW wind turbine tower. Its behaviour under seismic excitation is evaluated, damage states are defined, and a framework is developed for determining the probability of damage of the tower at varying seismic hazard levels. Results of the implementation of this framework in two Canadian locations are presented herein, where the risk was found to be low for the seismic hazard level prescribed for buildings. However, the design of wind turbine towers is subject to change, and the design spectrum is highly uncertain. Thus, a methodology is outlined to thoroughly investigate the probability of reaching predetermined damage states under any seismic loading conditions for future considerations.

Key words: steel structure, wind turbine tower, tubes, finite element analysis, seismic analysis, incremental dynamic analysis, fragility curve.

Résumé : La réponse sismique des tours d'éoliennes en tubes d'acier est une question importante puisque ces dernières sont de plus en plus installées dans zones sismiques et que les codes de calculs ne traitent pas clairement de cet aspect de la conception. Les aléas sismiques sont ainsi évalués pour l'environnement sismique canadien en utilisant une analyse implicite par éléments finis et une analyse dynamique incrémentielle pour une tour d'éolienne de 1,65 MW. Son comportement sous une excitation sismique est évalué, les dommages sont définis et un cadre est établi pour déterminer la probabilité de dommages à la tour à différents niveaux d'aléas sismiques. Les résultats de l'implantation de ce cadre en deux endroits au Canada sont présentés, où le risque était faible pour le niveau d'aléas sismiques prescrit pour les bâtiments. Toutefois, la conception des tours d'éoliennes est sujette à changement et la plage de conception est très incertaine. Ainsi, une méthode est présentée afin d'examiner en détail la probabilité d'atteindre des niveaux de dommages prédéterminés sous des conditions de charge sismique possibles dans l'avenir.

Mots-clés : structure d'acier, tour d'éolienne, tuyaux, analyse par éléments finis, analyse sismique, analyse dynamique incrémentielle, courbe de fragilité.

[Traduit par la Rédaction]

Introduction

Tubular steel monopole towers are the most common type of supporting structure for wind turbines in the world today. The increasing production of wind energy in North America has led to installation of these structures in areas where additional loading conditions, for which the tower was not initially designed, may exist. As some international design codes are being adopted in Canada for the design of these structures, several gaps are evident due to Canada's unique environment. One such gap is the assessment of seismic

risk pertaining to wind turbine towers, as the major developments of wind turbines have been in non-seismic areas. Their very tall and slender geometry results in a structure that cannot respond in a ductile manner, thus the capacity of wind turbine towers when subjected to dynamic seismic loads must be characterized, to ensure that they are not overloaded in such loading conditions.

Existing code provisions are few (IEC 2005; CSA 2008), and current research has thus far established that seismic loads typically do not govern the design of the tower (Bazeos et al. 2002; Lavassas et al. 2003). However, the seismic risk of wind turbine towers is still of importance to owners of wind turbine developments, especially wind turbine farms, because all the towers are generally identical, and as such, a seismic event would affect all the towers in the same manner — if one tower fails, they would all fail. Such a failure would result in severe financial losses as well as social implications if wind energy takes over more of the energy production in Canada. Thus, a methodology is presented herein for determining the probability of damage for a wind turbine tower at various levels of damage using the finite element method (FEM).

Received 19 April 2010. Revision accepted 10 January 2011. Published on the NRC Research Press Web site at cjce.nrc.ca on 8 February 2011.

E. Nuta, C. Christopoulos,¹ and J.A. Packer. Department of Civil Engineering, University of Toronto, 35 St George Street, Toronto, ON M5S 1A4, Canada.

Written discussion of this article is welcomed and will be received by the Editor until 31 July 2011.

¹Corresponding author (e-mail: c.christopoulos@utoronto.ca).

Code provisions

The most significant international standards for design of wind turbines are produced by the International Electrotechnical Commission (IEC), Germanischer Lloyd (GL), and Det Norske Veritas (DNV). The standards from GL and DNV, as well as other European standards, have been harmonized with the IEC standards. The Canadian Standards Association (CSA) has recently adopted the principal IEC standard for wind turbines, IEC61400-1 (IEC 2005), while including Canadian deviations that mostly concern external conditions to which the wind turbine may be exposed (CSA 2008).

The seismic provisions in IEC61400-1 require that a seismic analysis be carried out depending on site-specific conditions, and earthquake assessment is not required in locations that are excluded by the local codes due to weak seismic action (IEC 2005). In locations where seismicity may be critical, the seismic loading must be combined with a significant specified operational loading that occurs frequently during the turbine's lifetime (IEC 2005). The seismic loading is based on the ground acceleration for a 475-year recurrence period with design spectrum requirements defined by the relevant local building codes (IEC 2005). Evaluation of seismic loads may be carried out either in the frequency-domain or in the time-domain. Furthermore, a simplified conservative approach to calculate the seismic loads is provided in Annex C of this standard, but this approach is only recommended if the tower is the only part of the wind turbine that will experience significant loading due to seismic action (IEC 2005).

The recently adopted CSA-C61400-1 (CSA 2008) only adds one seismic provision to the IEC (2005) specifications. It acknowledges that the NBCC (2005) does not address earthquake forces acting vertically, and identifies this as a problem because wind turbines may have vibration modes with significant mass participation factors in the vertical direction (CSA 2008). Additionally, a discrepancy arises in the recurrence period of the seismic event to be used in design. The IEC61400-1 (IEC 2005), and thus the new CSA-C61400-1 (CSA 2008), suggests a 475-year recurrence period, whereas the NBCC (2005) defines seismic loading based on a 2500-year return period.

Pertinent research

The majority of current relevant research has been concerned with verifying that a given wind turbine can sustain low or moderate seismic loadings safely, without assessing the seismic capability limits of wind turbine towers. At fairly low seismic loads, Bazeos et al. (2002) concluded that seismic analysis does not produce the governing design criterion for this type of structure, and Lavassas et al. (2003) found that the seismic response was significantly less critical than the response caused by wind loading.

Much focus has also been on comparisons of frequency-domain and time-domain methods of seismic analysis, as it has become feasible to incorporate time-domain analyses in simulation packages for wind turbines, such as GH Bladed (Witcher 2005) and Flex5 (Ritschel et al. 2003). Witcher (2005) concluded that both methods were adequate, but discrepancies arose when the system damping was not close to that of the design spectra, which is typically 5%. For operat-

ing wind turbines, the total damping is close to 5% due to significant aerodynamic damping and thus both methods yield similar results (Witcher 2005). For turbines that are not operating, the aerodynamic damping, and thus the total damping, is much lower. Most building codes do not provide a method to correct for the level of damping when using the frequency-domain method, so the time-domain method is advantageous because the correct level of damping can be applied (Witcher 2005). Therefore, Witcher (2005) concluded that time-domain seismic analysis is acceptable, and in fact preferred, because the correct aeroelastic interaction can be modelled. A similar investigation by Ritschel et al. (2003) concluded that both methods are adequate for obtaining tower forces, but that the time-domain method was preferred for nacelle and rotor loads, which were significantly influenced by the vertical earthquake component.

Recent research has also addressed the effect of soil-structure interaction (SSI) when assessing the seismic resistance of wind turbines. Although the wind turbine tower was identified as the most important structural component when analyzing dynamic response (Zhao and Maisser 2006), the interaction between the structure, the foundation, and the surrounding soil was also considered to be significant (Bazeos et al. 2002; Zhao and Maisser 2006). For a weak earthquake load combined with design wind loading, Zhao and Maisser (2006) found that the peak tower displacement was dominated by wind forces. The inclusion of SSI resulted in reduced fundamental frequencies of the wind turbine. Thus, it was concluded that soil-structure interaction has a large influence on the dynamic characteristics of the wind turbine tower, particularly in areas with flexible soil, and this interaction should be included in dynamic analysis of wind turbines (Bazeos et al. 2002; Zhao and Maisser 2006).

Numerical analysis: development and validation

As the methodology established herein is based on numerical modelling using ANSYS Multiphysics (2007), several verification analyses were carried out to evaluate element formulations, mesh size and material properties, and to verify local and global failure mechanisms. The finite element (FE) model that facilitated the majority of the verifications was that of a short tubular member in pure flexure.

Elements

The wall of the tower was represented with 8-noded shell elements, and the ring flanges of the wind turbine tower were modelled using 20-noded solid elements. Both elements are well suited to model curved boundaries, as they have a mid-side node. A mesh sensitivity analysis of the pure flexure model indicated that an element size up to approximately 12 times the thickness satisfactorily captured the pure flexure response. Coarser mesh sizes captured the pre-peak response, but not the post-peak response.

Tubular members in bending

Flexural member cross-sections are classified by many codes based on their slenderness, which governs a section's ability to carry moment (AISC 2005; CEN 2005; CSA

Fig. 1. Properties of 1.65 MW wind turbine tower.

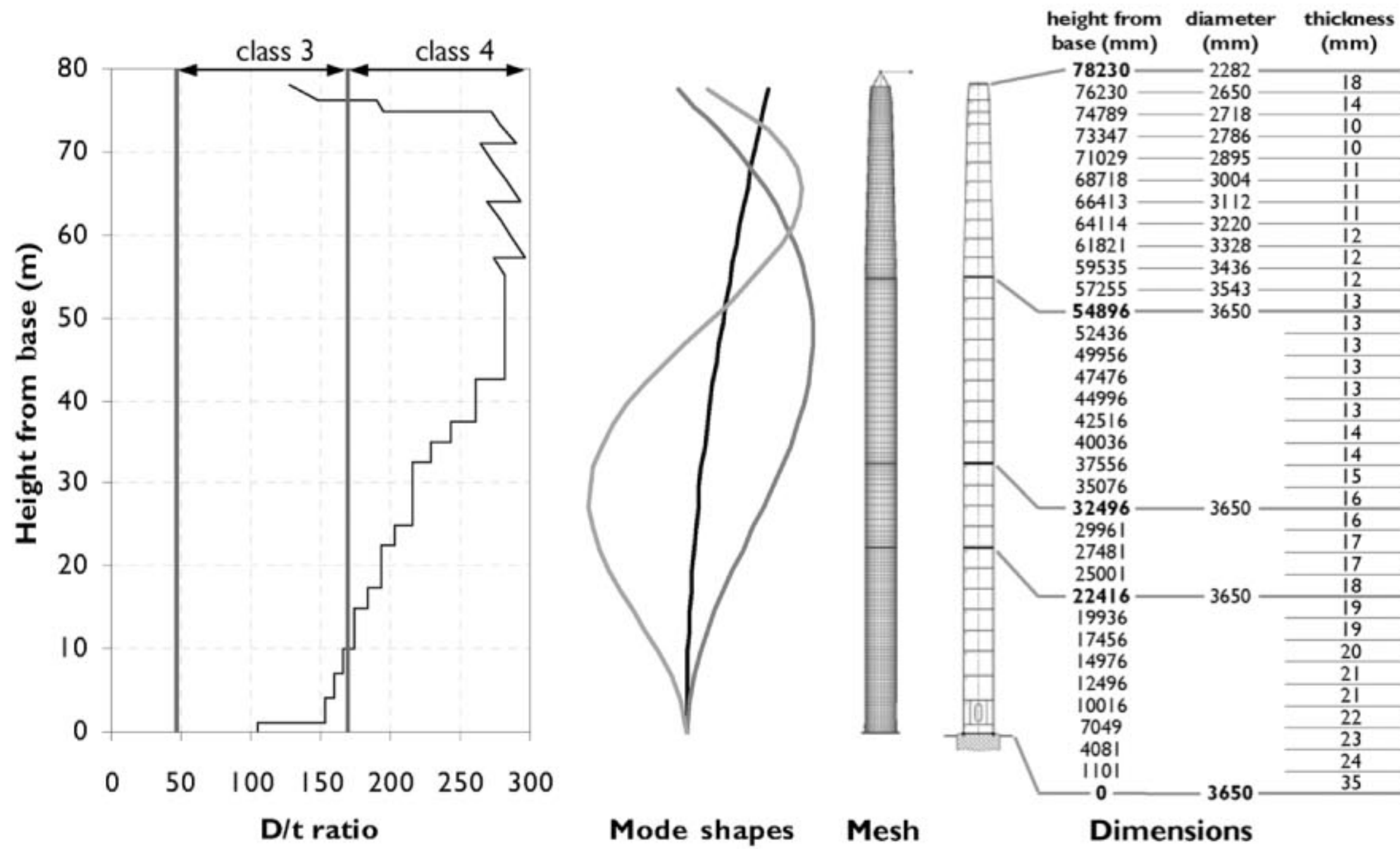
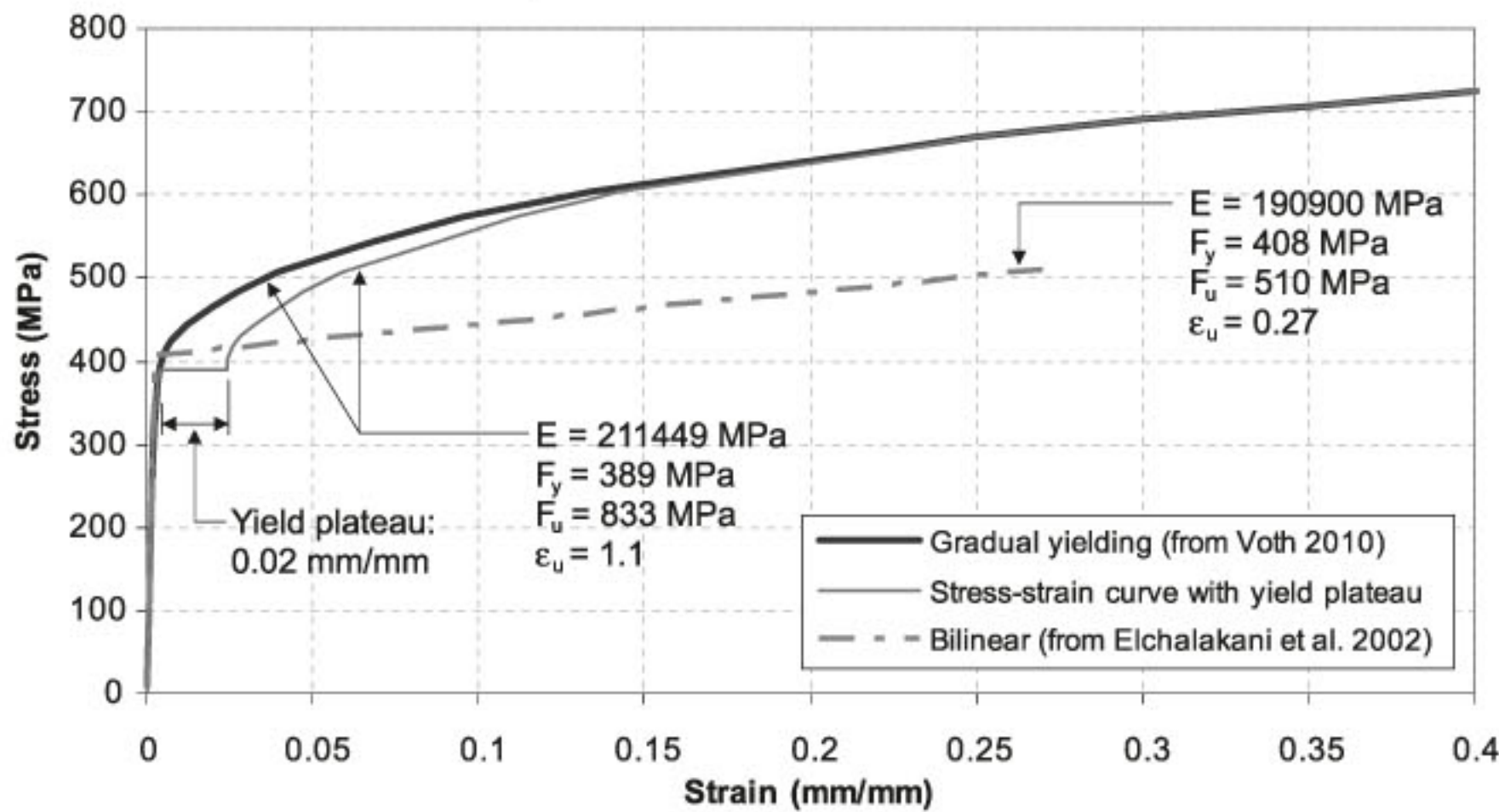


Fig. 2. True stress-strain curves used in verification analyses.



2009). If elements of the cross-section that are in compression are too slender, the flexural member may buckle locally instead of reaching its global flexural capacity. Sections of wind turbine towers fall within the realms of class 3 and class 4 in bending, where class 4 is defined as slender. This definition varies considerably between various codes. The bottom part of the specific wind turbine tower considered later in this paper is class 3 in flexure according to CSA S16, while most of the tower's height is well past the class 3 limit and is hence class 4 (Fig. 1).

Material properties

Typical steel wind turbine towers are made from flat steel plates that are rolled into cylindrical or conical pieces, and then welded longitudinally (Danish Wind Industry Association 2003). Due to this fabrication process, the material properties of the tower are similar to cold-formed tubular members. The stress-strain curve of the material shows a

low proportional limit, followed by gradual yielding, no clear yield plateau, and significant strain hardening.

No material data in the form of stress-strain behaviour from an actual wind turbine tower was available. For the verification analyses, three sets of material properties were used (Fig. 2): gradual yielding, taken from the average of several coupon tests of cold-formed circular HSS sections performed by Voth (2010); stress-strain curve with yield plateau, adapted from Voth (2010); and bilinear stress-strain, obtained from Elchalakani et al. (2002).

Finite element comparison with experimental specimen

An FE model of geometrically-comparable ratios to an experimental specimen from Elchalakani et al. (2002) was carried out. The response curve shape was similar, but the agreement was not ideal as the peak was over-estimated by 9% (Fig. 3). This is believed to be due to imperfections in the experimental specimen. In addition, the FE model used

Fig. 3. Response of FE model VF-el compared with experimental results from Elchalakani et al. (2002).

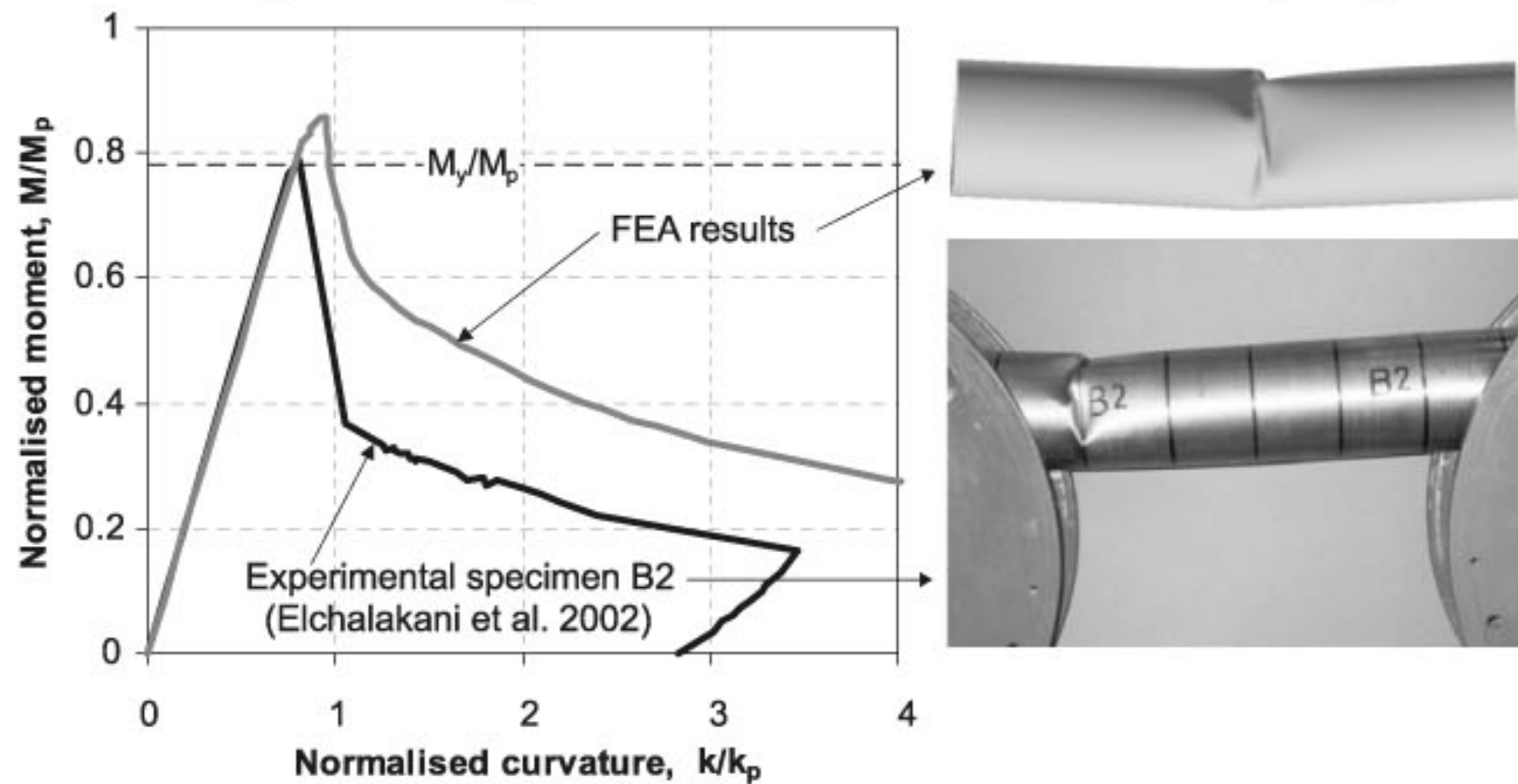
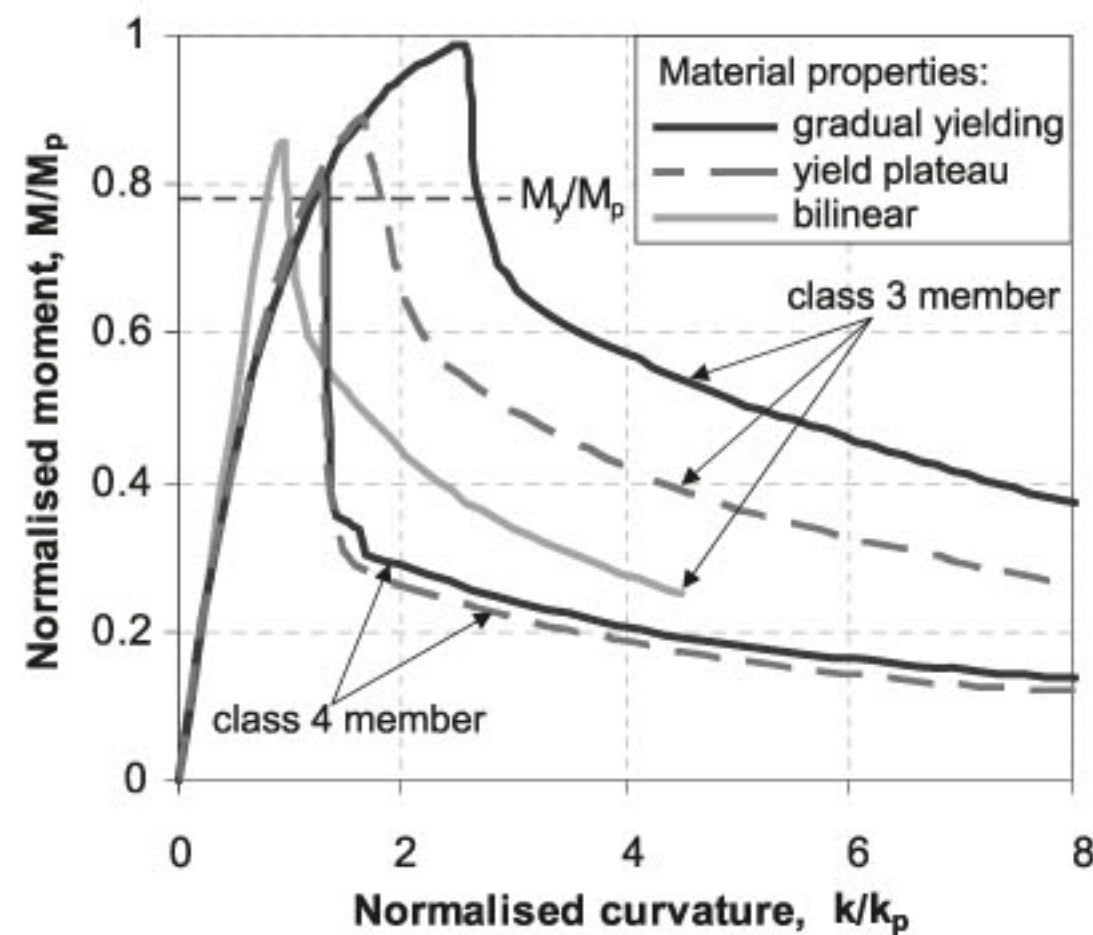


Fig. 4. Effect of material properties on pure flexure response.



an assumed bilinear stress-strain curve, since the true stress-strain curve was not reported by Elchalakani et al. (2002). Despite these differences, the buckling failure mode was captured well (Fig. 3).

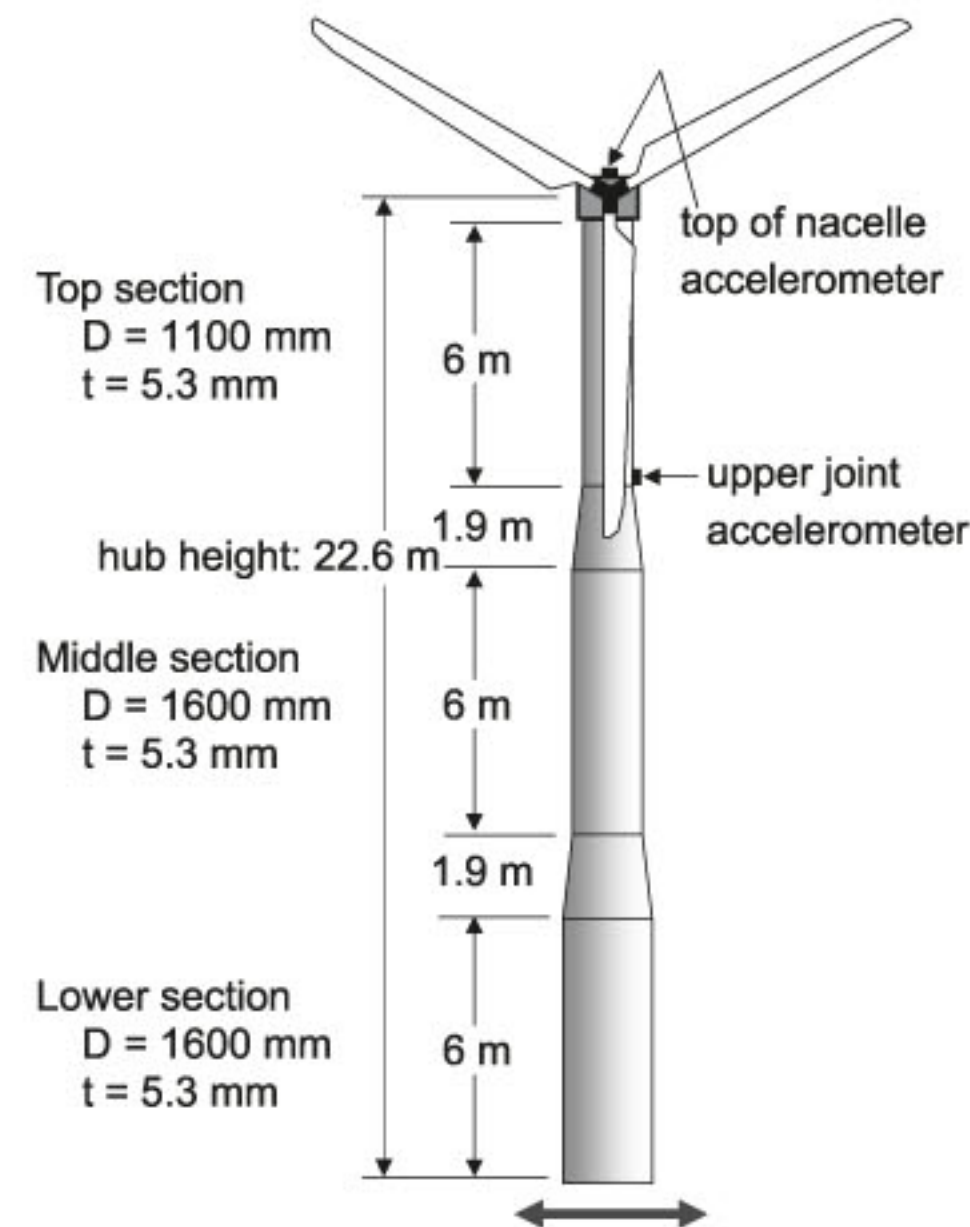
Effect of material properties

Two pure flexure models, class 3 and class 4, were used to assess the effect of material properties on flexural response (Fig. 4). For the class 3 member, the presence of a yield plateau in the stress-strain curve influences how early the member buckles, whereas the behaviour of the class 4 member is almost unaffected by the material properties. For the subsequent analyses, the gradual yielding stress-strain curve was employed. The material properties were kept constant for all subsequent analyses and thus the uncertainty related to these properties was not considered in this study. It was deemed that material uncertainty would be insignificant when compared to the uncertainty related to the input ground motions.

Analysis of small wind turbine tested at UCSD

A full-scale shake table test of a small wind turbine was carried out at the University of California, San Diego (Prowell et al. 2008 and 2009). The turbine was 22.6 m tall and consisted of three sections of constant cross-section con-

Fig. 5. Details of small wind turbine tested at UCSD.



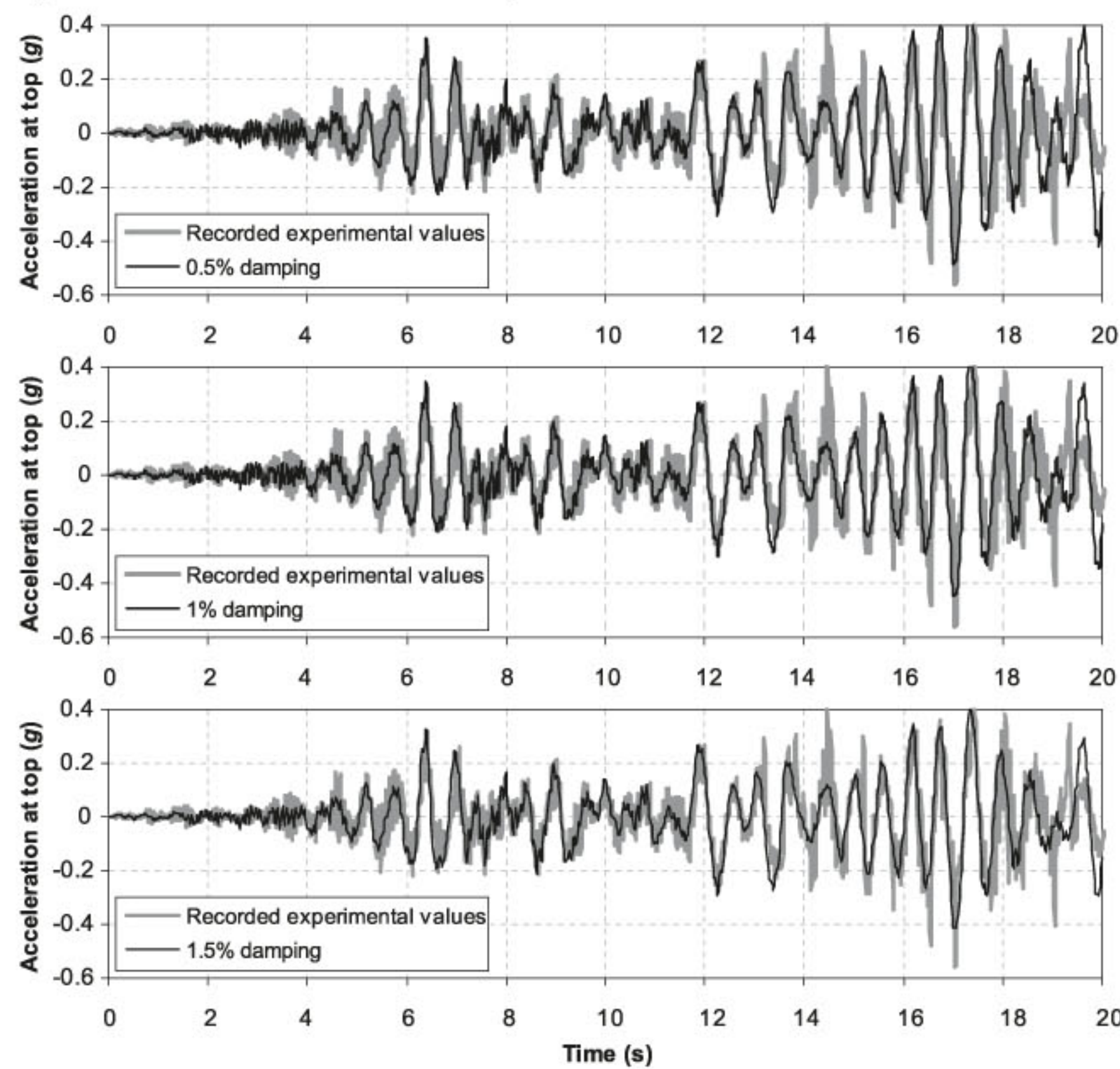
nected by conical joints (Fig. 5). A simple FE model was created using shell elements and additional mass elements, uniformly distributed throughout the tower, to reach the mass specified by Prowell et al. (2008). Modal analysis estimated the first modal period to be 0.58 s, which was in good agreement with the experimentally observed first mode of 0.59 s (Prowell et al. 2008).

The model was subjected to the same ground motions as the shake table test corresponding to the results presented in Prowell et al. (2008), 143% of the east-west component of the 1992 strike-slip Landers Earthquake. More recently, Prowell et al. (2009) presented results for the 100% and 200% level of the Landers earthquake, but the FE analyses discussed herein were compared to the 2008 publication. The ground motion record, obtained from the US Geological Survey database, was 80 s long, and the analyses had an additional 15 s of free vibration.

Comparison of effect of damping

Based on experimental results, Prowell et al. (2008) calculated the amount of viscous damping to be between 0.4% and 0.6% of critical for the small wind turbine described

Fig. 6. Finite element and experimental values: acceleration at top of nacelle.



above. This is similar to the estimated value of 0.5% used by Bazeos et al. (2002) in their dynamic analysis of a wind turbine. However, industry guidelines suggest the use of 1% of critical damping for a parked wind turbine (blades locked against motion) (IEC 2005).

Rayleigh damping was specified in the FE analyses to obtain 0.5%, 1%, and 1.5% of critical damping for the first and second modes. The FE results and the experimental results are plotted for the acceleration at the top of the nacelle and at the upper joint, respectively, for the first 20 s of the earthquake (Fig. 6 and Fig. 7). This duration was chosen to allow for a comparison with the results presented in Prowell et al. (2008).

The agreement between the FE results and the experimental results is reasonable, considering all the simplifying modelling assumptions — uniform distribution of additional mass, no modelling of the blades, and rigid fixity at the base. Prowell et al. (2008) presented better agreement in their publication from a numerical model wherein the parked blades were included using beam elements. This suggests that modelling the blades changed the higher mode effects and thus affected the response of the upper joint, which is dominated by the higher modes. However, no details of the blades were available, thus the influence of the blades cannot be assessed.

Comparison of the FE results and the experimental results shows that the nacelle response is better captured using lower damping, while the upper joint response is better represented by higher damping. A damping value of 1% of critical was chosen for seismic analysis of further wind turbine

towers, as a compromise between achieving the best match for the nacelle response and for the upper joint response.

Properties of typical wind turbine tower model

A typical 1.65 MW wind turbine tower is analyzed in this paper, with a diameter and thickness that ranges from 3650 mm and 35 mm at the base to 2282 mm and 10 mm at the top, respectively (Fig. 1). The finite element model has a fine mesh (element size to thickness ratio of 12) with a good aspect ratio in the bottom section of the tower, where buckling failure typically occurs. The model also includes two openings at the base: a door and a cable hole. Holes are left in the tower FE shell where the actual door and cable holes are located. The door section covers 1/6 of the tower's circumference and is approximately twice as thick as the rest of the wall at that height in the tower. The bottom section, where the cable hole is located, is already quite thick (35 mm) and there is a lip around the hole. It is important to include these details, as they may affect the response of the tower.

Modal analysis of the tower calculated the fundamental frequency to be 3.17 s. The first three modes in the horizontal direction are shown in Fig. 1.

Pushover analysis

Pushover analysis is a simplified inelastic analytical procedure developed to estimate the seismic response of structures. Many pushover procedures have been developed and

Fig. 7. Finite element and experimental values: acceleration at upper joint.

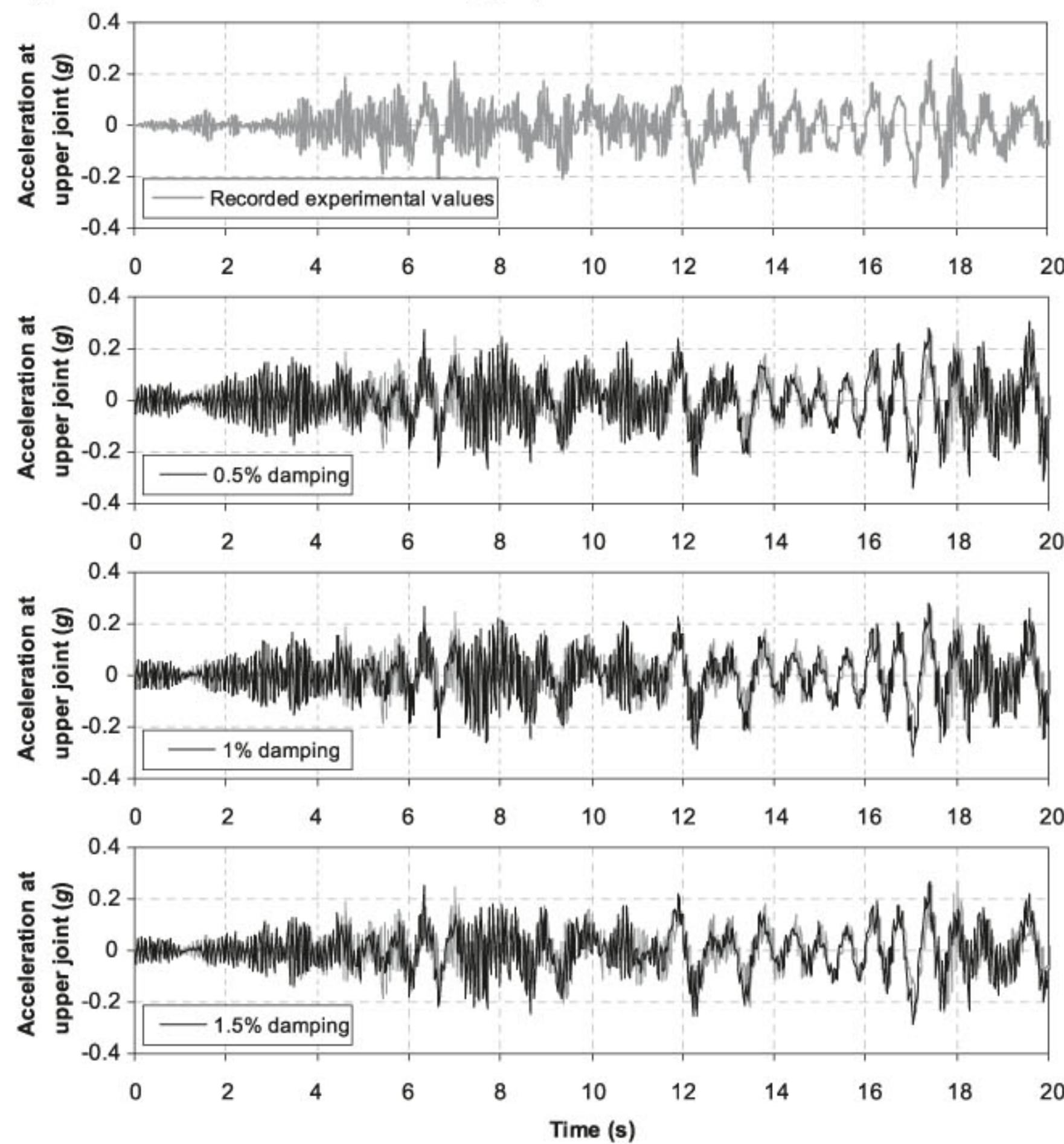
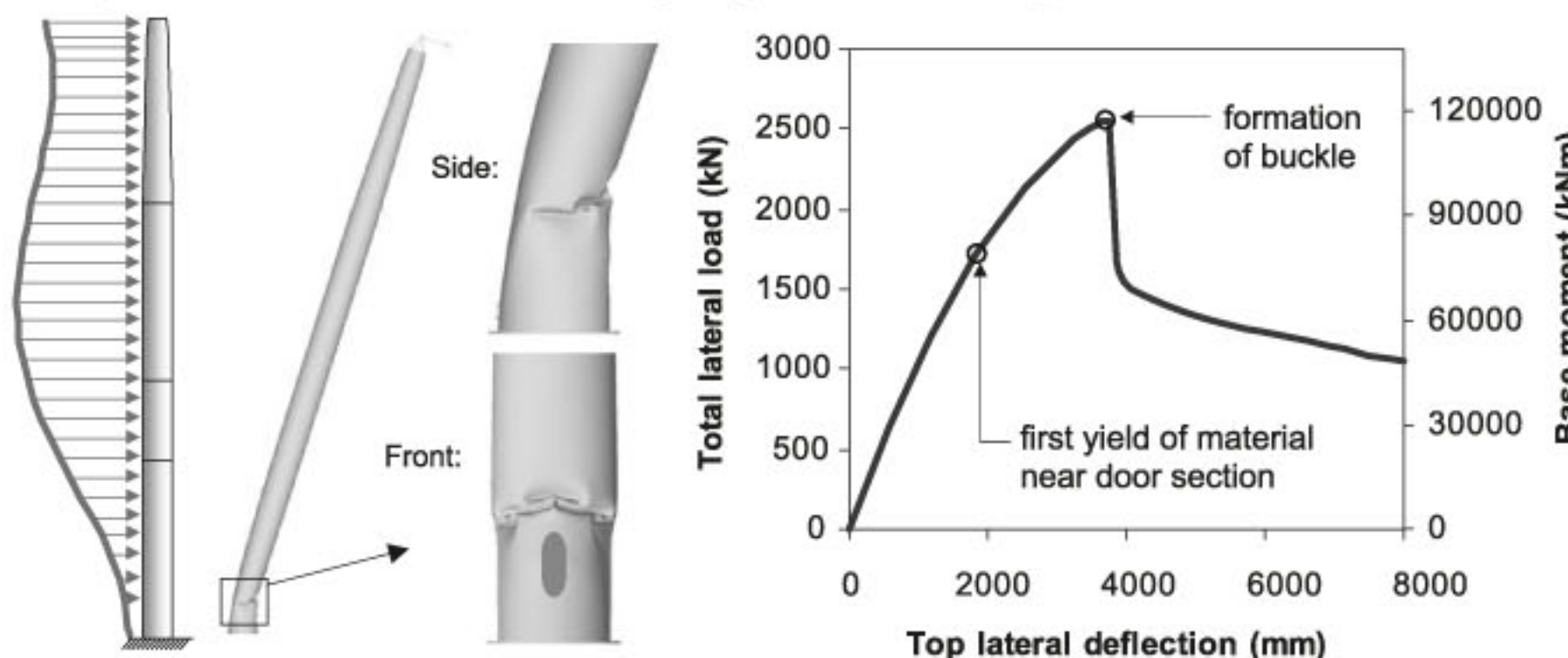


Fig. 8. Pushover analysis load pattern, buckled failure, and capacity curve at 0° angle.



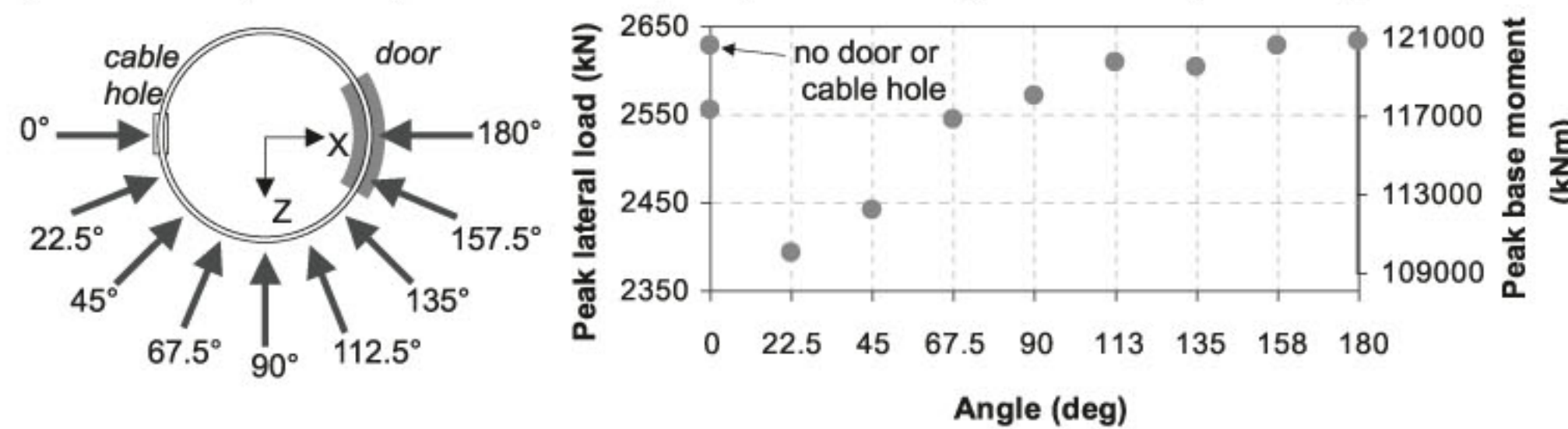
validated for particular types of buildings and bridges, but none have been tailored for a structure similar to a wind turbine tower. As such, a simple multimode load pattern (Barros and Almeida 2005) was used to determine the capacity of the tower and to assess its behaviour. The load pattern consisted of a linear combination of the first three modes in the horizontal direction, as follows:

$$[1] \quad LP = \sum \alpha_i \phi_i$$

where LP = load pattern; α_i = modal participation factor of mode i ; ϕ_i = mode shape of mode i , normalized to mass matrix.

The resultant force of the load pattern (Fig. 8) acts at 45.9 m above the ground. The pushover analysis was carried out at 22.5° increments around the circumference of the tower (Fig. 9) to determine the weakest angle of incidence. The capacity curve of the pushover analysis at an angle of 0° (Fig. 8) was similar to that of the pure flexure specimens: nearly-linear response until yield, followed by slightly curvilinear response until the peak, where a buckle formed and the tower quickly shed the load. The response at various angles of incidence was very similar (Fig. 9), but the peak load varied slightly, with the lowest peak load being achieved when the angle of incidence was 22.5° , followed by 45° . This is believed to be the case because the compression

Fig. 9. Directions of pushover analyses in top view of tower, and peak load for pushover analyses acting at various angles.



side is very close to the corner of the thickened tower door section, so stress concentrations for those analyses are almost exactly at the location where the buckle forms, thereby causing failure earlier than when the tower is pushed in any other direction. In addition, one pushover analysis was carried out without modelling the door and cable hole at the bottom of the tower and, as expected, these details are indeed necessary in the model of the wind turbine tower. The most significant result of the pushover analyses is the buckled failure of the tower (Fig. 8). As expected, the failure occurs close to the base, but above the thickened door section.

Time-history analysis

The described model was subjected to time-history analysis by applying orthogonal earthquake components at the base of the tower as displacement ground motion records. At the end of the record, the analyses were continued for an additional 60–65 s of free vibration until the tower's oscillations diminished to near zero. The buckling failure of the wind turbine tower during seismic excitation typically occurred at either 10 m above the base or around 43 m above the base. This is a different location from that obtained in the pushover analyses, where the failure occurred much closer to the base, just above the stiffened door section. This difference is due to the effect of higher modes in the dynamic seismic response of the structure.

Effect of damping

The wind turbine tower's sensitivity to damping was assessed by running one seismic event with varied damping values: 0.5%, 1%, and 1.5% of critical, at magnification factors 1, 2, and 4. The peak and pre-peak response was not heavily influenced, especially as the magnification factor was increased. However, the post-peak time-history response of the wind turbine tower was significantly influenced by the amount of damping. Nonetheless, the resulting residual displacement was almost identical between the various damping values, although the analyses with lower damping oscillated for much longer in free vibration before the tower came to rest.

Effect of vertical acceleration

The vertical earthquake component of one seismic event was included to determine the extent to which it affects the response of the wind turbine tower at magnification factors 1, 2, and 4. The peak vertical ground acceleration was $0.723g$, almost as high as one of the horizontal components. Thus, the vertical component for this particular earthquake record is quite significant.

Despite including such a significant vertical earthquake component, the response of the tower was barely affected. This is because the normal stress created in the tower's bottom section under gravity loads is small (less than 10%) compared to the normal stress in the same section due to bending for the reference earthquake (magnification factor = 1).

Incremental dynamic analysis

The typical 80 m tower supporting a 1.65 MW turbine was subjected to incremental dynamic analysis (IDA) to assess its response to seismic loading. Intensity measures and damage measures are required to extract information from the IDA, and damage states of interest must be characterized.

Intensity measures

The intensity measures are commonly the peak ground acceleration or the peak ground velocity (Vamvatsikos and Cornell 2002). The intensity measure is chosen such that the dispersion of all the incremental time-history analysis curves is minimized. For the IDA of the wind turbine tower, the intensity measure employed was the magnification factor. Since all the earthquakes were chosen to represent the design response spectrum, the magnification factor represents the intensity of the ground motion with respect to the intensity of the design earthquake. Other intensity measures investigated were the peak ground displacement, the peak ground velocity, and the peak ground acceleration, but the dispersion of the IDA curves was smallest when the magnification factor was used as the intensity measure, followed closely by the peak ground velocity.

Damage measures

The damage measure is typically the peak roof drift of a structure (Vamvatsikos and Cornell 2002). Several damage measures were considered: the peak displacement, the peak rotation, and the residual displacement. The peak stress was also investigated.

Peak displacement

For each analysis, the displacement at hub height in three orthogonal directions (x , y , and z) was obtained for each time increment throughout the analysis. The resultant displacement was computed based on the two lateral displacements, and the maximum displacement was thus obtained for each analysis. The peak lateral displacement (Δ_{\max}) is described as a percentage of the hub height.

Peak rotation

The peak rotation of the tower, θ_{\max} , was computed at a specific time through the analysis, typically at the time the peak displacement occurred.

The rotation was calculated as the relative angle of 32 segments that correspond to the pieces of the tower (Fig. 1). These segments were employed in defining the peak rotation to simplify the post-processing analysis, but the tower may be evenly divided into segments that are approximately 70% of the tower's diameter at the base. Furthermore, the displacement of the tower at each location along the height was taken as the average of 12 evenly spaced points around the circumference at that elevation, ensuring that the deformed shape represented the centreline of the tower and was not influenced by any ovalisation that may have occurred.

For analyses where buckling occurred, the rotation of the segments very close to the buckle was not considered accurate due to local crumpling of the shell on one side and flattening of the tower wall on the side opposite the buckle. Two or three segments were thus ignored in calculating the rotation for analyses that buckled. The centrelines of the two segments without severe deformation that bracketed the buckled area were extrapolated and the relative rotation between these two extrapolated lines was taken as the peak rotation.

Peak stress

The peak stress considered was the peak von Mises stress (σ_{mises}). Prior to buckling, the peak stress typically occurred at the side of the door hole opening on the inside of the tower. In the incremental analyses where the tower buckled, the peak stress was typically at the location of the buckle.

Residual deformation

The residual lateral deformation (Δ_{res}) at hub height is stated as a percentage of the hub height. In most cases, there was a small residual displacement even after analyses where the peak stress did not exceed the yield stress of the material ($F_y = 389 \text{ MPa}$). This occurred because the stress-strain curve is slightly curvilinear until nominal yield, due to the material properties being assumed to be similar to those of a cold-formed tubular member.

Damage states

Limit states are typically defined using prescribed values to ensure safety of occupants and stability of buildings. However, wind turbine towers do not fall in the same category as buildings, as they are generally not occupied. In the absence of clearly defined limit states for seismic performance assessment of wind turbine structures, several damage measures were defined for this study. It was deemed that these damage states would be related to the functionality and the cost of repair of wind turbines following a major earthquake.

0.2% residual out-of-straightness

The acceptable out-of-straightness for wind turbine towers is not well defined, but this value for other structures varies in Canadian standards between 0.1% (CSA 2004, 2009) and 0.2% (CSA 2001). This out-of-straightness is typically de-

fined for erection purposes. As there is some residual deformation before the yield stress is reached due to the curvilinear material properties, an out-of-straightness limit of 0.1% was considered to be too severe. For this study, a residual out-of-straightness of 0.2% was taken as the first damage state. Linear interpolation between the two analyses that enveloped a residual displacement of 0.2% of hub height was carried out to determine the damage and intensity measures at this damage state.

First yield

Linear interpolation between the two analyses that enveloped a peak yield stress, $F_y = 389 \text{ MPa}$, was carried out to define the values of the second damage state.

1.0% residual out-of-straightness

Yielding of the tower typically falls within 0.2% residual out-of-straightness (the first damage state) and 1.0% residual out-of-straightness. Due to the uncertainty of the material properties of the wind turbine tower, this damage state was investigated as well. Similar to the previous two damage states, linear interpolation was employed to obtain the values that define 1% residual out-of-straightness.

First buckle – loss of tower

The last damage state corresponds to the first incremental analysis that causes the tower to buckle. The wind turbine tower is considered as a complete loss after this damage state is reached, given the fact that the sections comprising the tower are class 3 or class 4. However, the tower is likely still standing after the first buckle is formed. For this damage state, there is no linear interpolation, and the lowest magnification factor that produces buckling of the tower defines the intensity and damage measures of this damage state.

Some of the incremental analyses were continued past the last damage state and a few buckled very severely. The FE model was able to capture buckling failure for all of the earthquakes, indicating a robust model.

Sites considered

Incremental dynamic analysis of the wind turbine tower was carried out for three locations: Los Angeles (LA), Eastern Canada, and Western Canada.

The LA earthquake suite is made up of 10 recorded earthquakes (20 records for the orthogonal components of the earthquake), compiled and scaled by Somerville et al. (1997). This suite of earthquakes is representative of earthquakes having a 475-year return period or a probability of exceedance of 10% in 50 years, and is defined as the design-based earthquake (ASCE 2005). The average spectrum of the 20 records is well matched to the design spectrum (Fig. 10).

For the Canadian sites, the uniform hazard spectrum was used to represent the design earthquake, as dictated by NBCC (2005), which corresponds to a 2500-year return period or a probability of exceedance of 2% in 50 years. The earthquake suites for these locations were based on databases of simulated earthquake time histories over a range of magnitudes, distances, and site conditions created by Atkinson (2009), who also outlines a method of selecting and

Fig. 10. Acceleration response spectrum for Los Angeles earthquake suite.

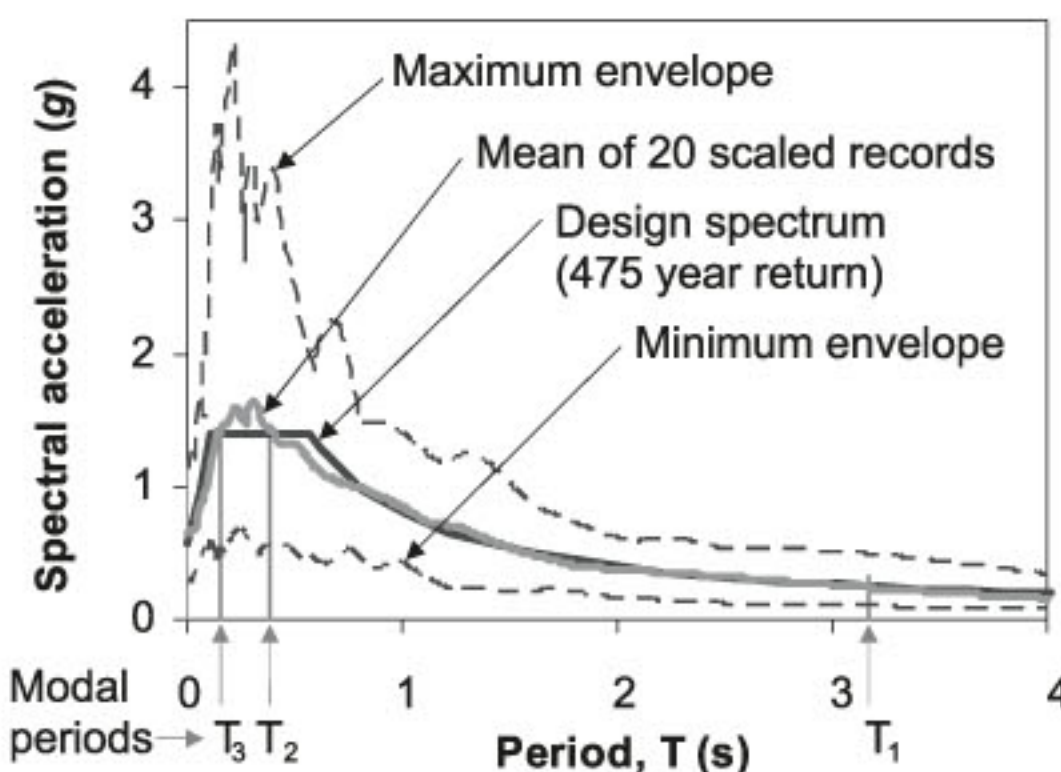
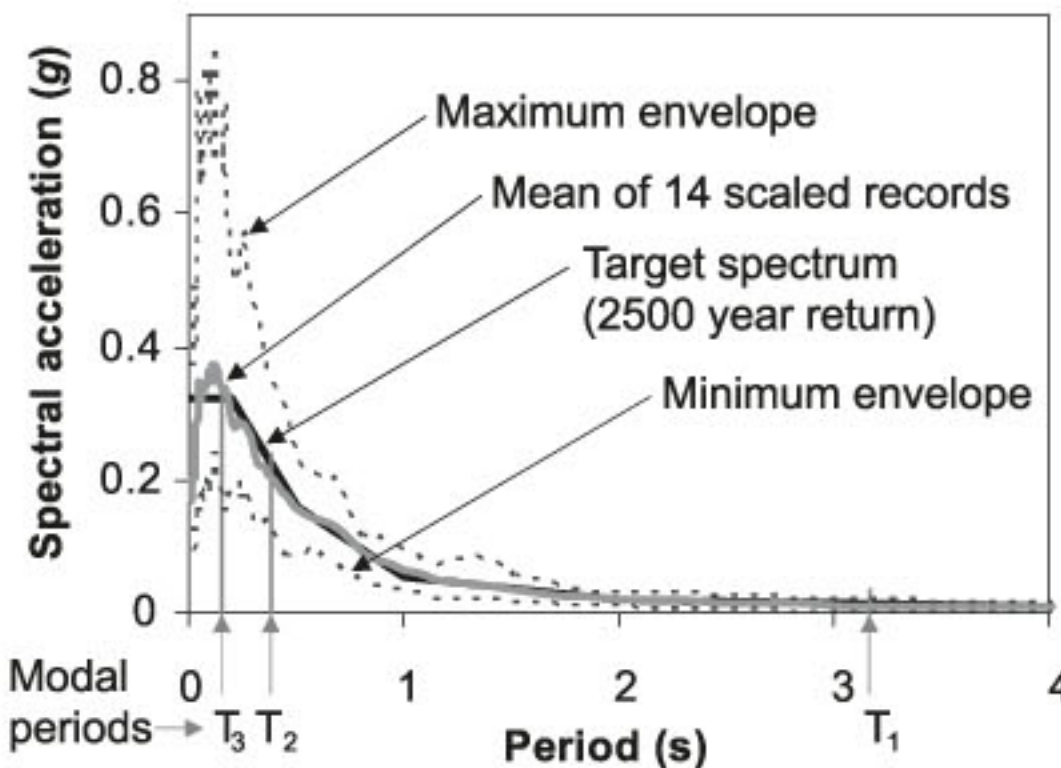


Fig. 11. Acceleration response spectrum for Eastern Canada earthquake suite.

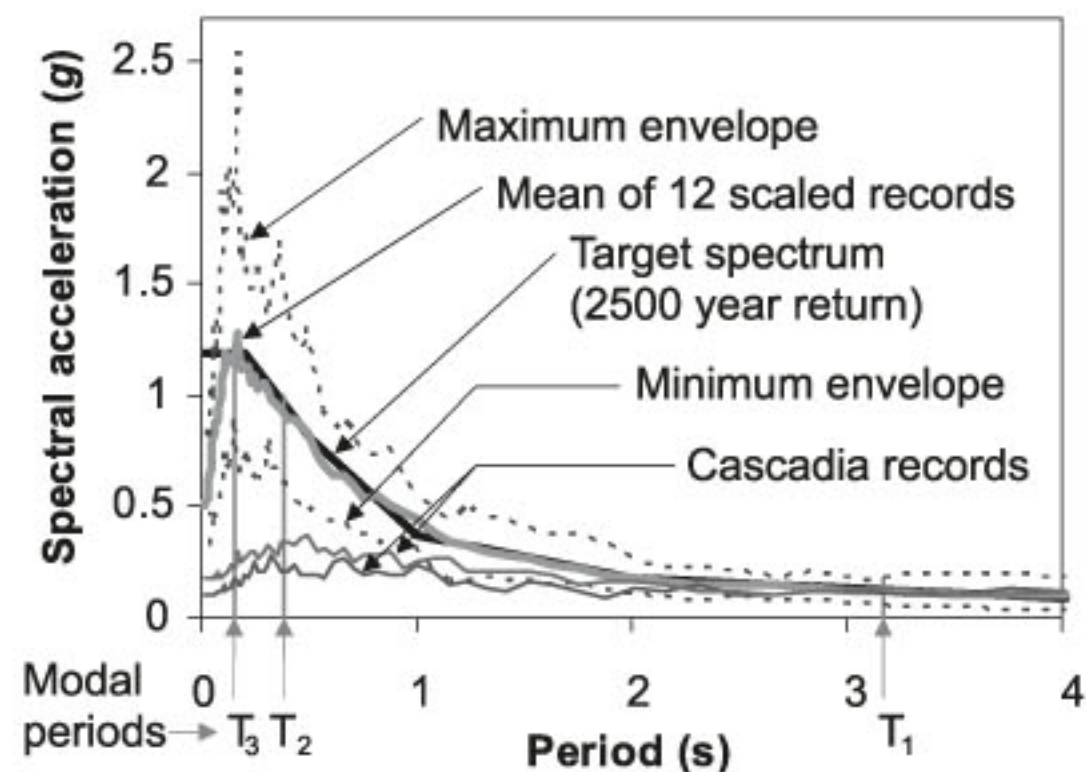


scaling records to create an appropriate suite. Each database was made up of several record sets of similar magnitudes and distances from which records can be selected.

The Eastern Canada location chosen was on the north shore of Lake Erie, south-west of Dunnville, Ontario. It is one of the locations close to Toronto, Ontario, currently being investigated for wind turbine farm developments. Due to the lower variability of simulated records, the Eastern Canada earthquake suite only comprised 7 earthquake records (14 orthogonal component records). The average spectrum of the 14 records is very closely matched to the uniform hazard spectrum of the area (Fig. 11).

The Western Canada location chosen was offshore just south of Victoria, BC. While that area is not under consideration for wind turbine developments to the authors' knowledge, it represents one of the most severe seismic hazards in Canada and was thus investigated in this paper. The earthquake suite for this site has six records from the database for Western Canada that had good agreement, on average, with the target spectrum (Fig. 12). In addition, a seventh earthquake, representing an event occurring on the Cascadia subduction zone, was also included in the study to assess the impact of such a large magnitude, large distance event on the seismic response of this wind turbine structure. As can be seen in Fig. 12, this event has lower spectral accelerations in the short period range but is in good agreement with the spectral accelerations of the target design spectrum for periods greater than 2 s.

Fig. 12. Acceleration response spectrum for Western Canada earthquake suite.



Method of scaling records

For each earthquake record, the initial analysis was the reference record that was matched to the target spectrum. The subsequent analyses aimed to reach the defined damage states. However, the predictability of the magnification factor required to reach any given damage state was found to be very low.

Fragility curves

Statistics of incremental dynamic analyses can be used to generate fragility curves, which serve the purpose of estimating the probability of reaching a defined damage state for a range of intensity values (Nasserasadi et al. 2008). The fragility curve is characterized by a lognormal distribution and thus employs the mean (μ) of the intensity measures and the standard deviation (σ) of the natural logarithms of the intensity measures (Deierlein et al. 2008). Using these statistics, the following lognormal distribution function defines the probability that the damage will exceed the damage state (DS) at a given intensity measure:

$$\begin{aligned} [2] \quad p(\text{damage} \geq \text{DS} | \text{IM}) \\ = \int_0^{\text{IM}} \frac{1}{\text{IM} \sigma \sqrt{2\pi}} \exp \left[-\frac{1}{2} \left(\frac{\ln(\text{IM}) - \ln(\mu)}{\sigma} \right)^2 \right] d(\text{IM}) \end{aligned}$$

Incremental dynamic analysis results

The IDA curves for the Los Angeles location and the Western Canada location are shown in Fig. 13 and Fig. 14, respectively. It is clear that the recorded earthquakes of the LA earthquake suite have much more variability. The simulated earthquakes of the Western Canada earthquake suite also have high dispersion, but earthquake records from the same record set have very low dispersion, as can be seen from the IDA curves for WCan02, WCan03, WCan04, and WCan05 (Fig. 14).

For the Eastern Canada location, it was found that the seismic response was very slight for the reference earthquakes. Analyses at a magnification factor of 10 produced a response that was well below the first damage state, and the predicted magnification factors to reach the first damage state ranged from 25 to 62. It was thus deemed that further analyses were unnecessary for this wind turbine tower at the

Fig. 13. Incremental dynamic analysis curves for the Los Angeles location.

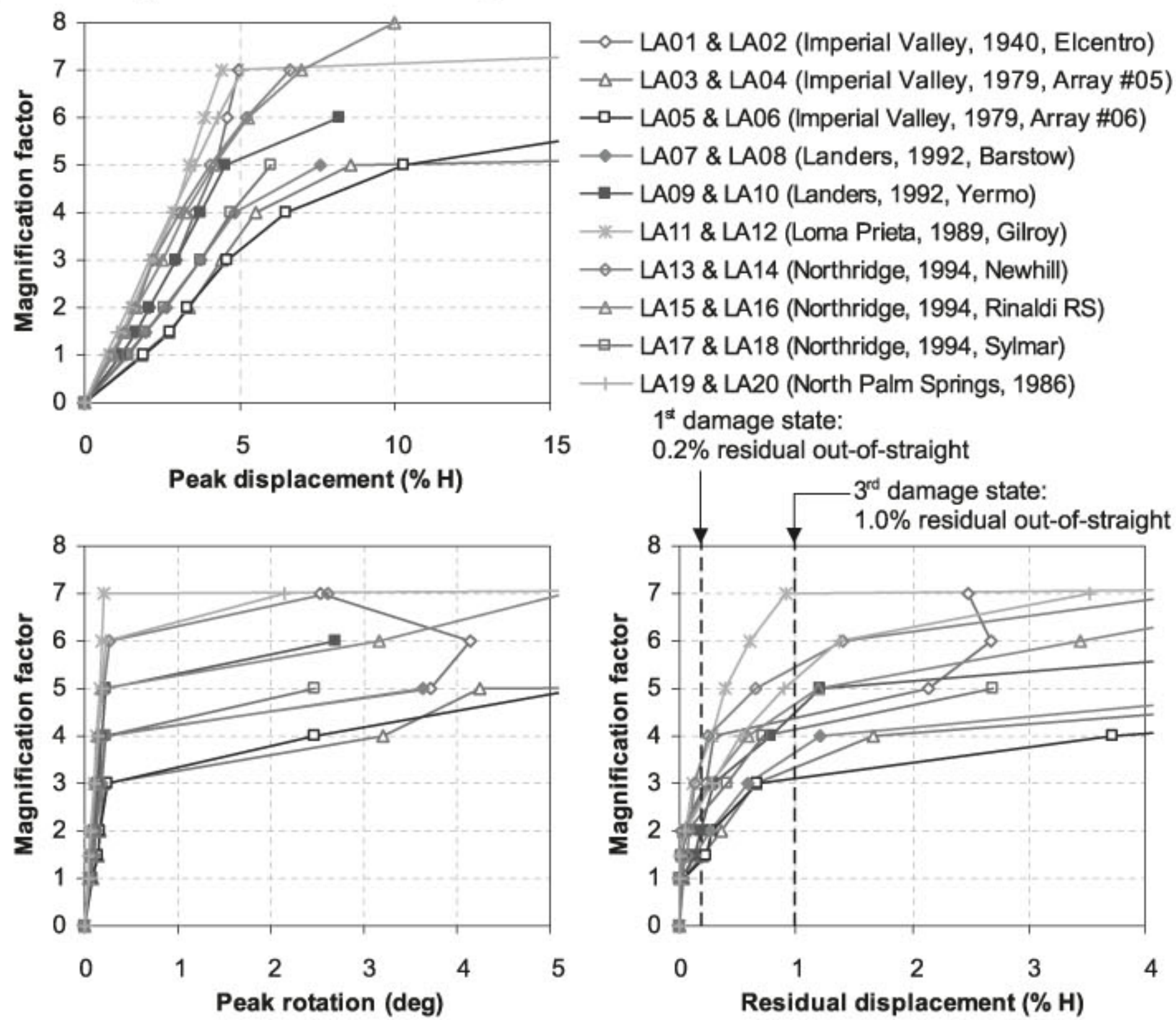
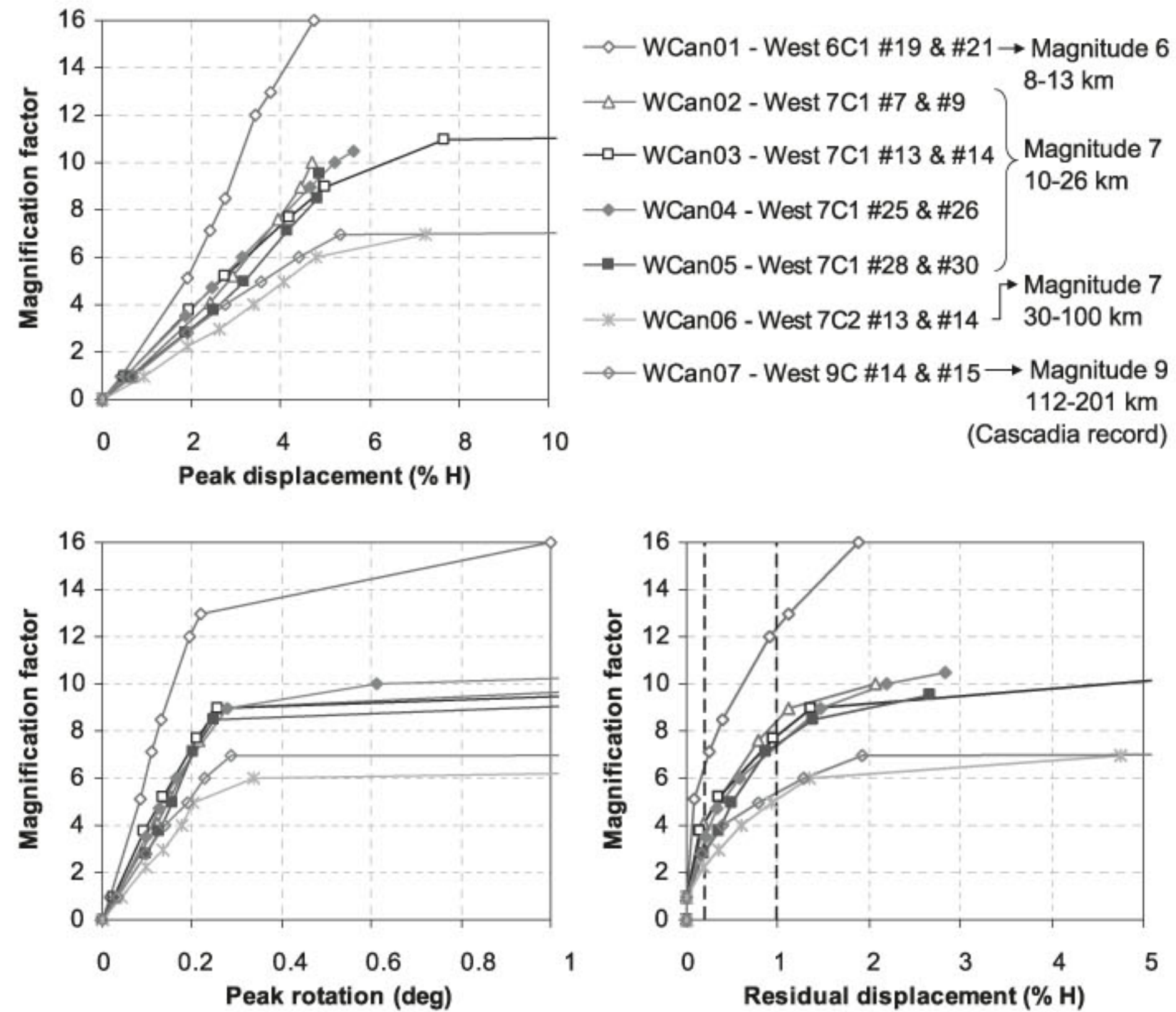
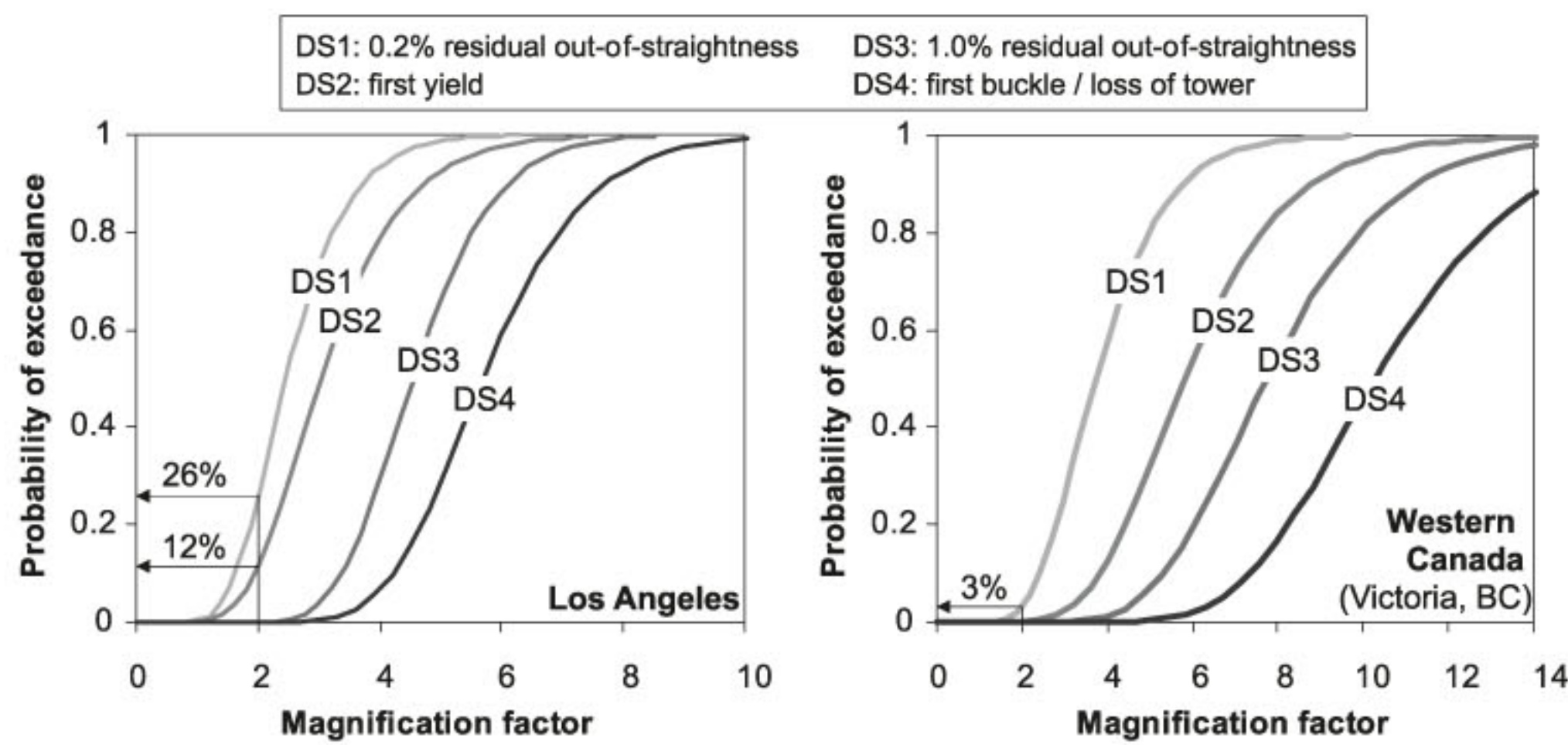


Fig. 14. Incremental dynamic analysis curves for the Western Canada location.



Eastern Canada location. However, given the high degree of uncertainty associated with this design spectrum and the extremely low spectral accelerations in the long-period range

that is relevant to the response of turbine towers, the seismic assessment of such structures should be carefully re-assessed as the seismicity of Eastern Canada is refined in the future.

Fig. 15. Fragility curves.

Assessment of damage measures

The peak rotation is a good damage measure because it indicates very clearly when buckling occurs. Although the response is not entirely linear up to that point, the increase in the peak rotation once buckling occurs is very drastic in every case.

The residual displacement is also important because it defines two of the damage states. Of the three damage measures, the residual displacement has the least dispersion, which is an important factor for IDA analyses.

The peak displacement appears to be the least indicative damage measure. There are a few analyses where the tower buckled yet the peak displacement IDA curves did not give any indication of this, depending on the height where the buckle formed.

Probability of exceeding the damage states

The resulting fragility curves for Los Angeles and Western Canada are shown in Fig. 15. A magnification factor of 1 represents the design earthquake for each location, which is 1 in 475 years for Los Angeles and 1 in 2500 years for Western Canada. Each curve can then be interpreted by choosing a magnification factor, i.e., the intensity of an event with respect to the design earthquake, and then using the curve to determine the probability of exceeding a particular damage state during an earthquake of that intensity.

The fragility curves (Fig. 15) show that the probability of damage of the 1.65 MW wind turbine tower during a seismic event is fairly low at both locations. Considering an event twice as intense as the design earthquake (i.e., magnification factor of 2), the fragility curves for LA indicate that there is 26% probability of exceeding the first damage state and 12% probability of exceeding the second damage state, while the fragility curves for the Western Canada location indicate that only the first damage state may be exceeded with a low probability of 3%. It is apparent that the seismic risk of wind turbine towers in Los Angeles is much greater than in Western Canada.

Conclusions

The behaviour of the tubular steel tower of a typical 1.65 MW parked wind turbine has been numerically investi-

gated under seismic loading, and its seismic risk was evaluated at three locations, two of which were in Canada. For this analysis, a finite element model of the steel tower was developed and thoroughly validated and the expected failure mode, buckling in flexure, was adequately captured. Earthquake suites were assembled and used to carry out nonlinear incremental dynamic analysis. Fragility curves were defined for four potential damage states of the wind turbine tower: 0.2% residual out-of-straightness, first yield at a stress concentration, 1% residual out-of-straightness, and first buckle. The results obtained represent the seismic hazard of the investigated wind turbine tower at the investigated locations. In the process of analyzing this typical wind turbine tower, a methodology for the seismic risk assessment resulting in fragility curves has been outlined, and may be applied to any tubular steel wind turbine tower subject to any level of seismic hazard.

The incremental analyses for either location in Canada (Victoria, BC and Southern Ontario) suggest that the seismic risk for the wind turbine tower that was investigated is very small. The seismic risk of this wind turbine tower in the Los Angeles area is much higher, although still not significant at the intensity level of the design earthquake. This is due to the long fundamental period of the tower and the short predominant period of most earthquakes.

However, the analyses presented herein demonstrated that these structures must be designed for large safety factors against any overloading, as they are prone to collapse when the tower is excited beyond its elastic limit. As the design of wind turbine towers is quickly evolving, with a tendency for taller structures, the seismic response may become more critical.

Acknowledgements

Financial support has been provided to the first author by Ontario Graduate Scholarships (OGS), the Natural Sciences and Engineering Research Council of Canada (NSERC), and the Steel Structures Education Foundation (SSEF). Also gratefully acknowledged are the Ontario Centres of Excellence (OCE) and the Fraunhofer Centre Windenergie und Meerestechnik, Bremerhaven, Germany, where the first author interned. Experimental shake-table data of the small wind turbine was provided by UC San Diego from a pilot

test series conducted under the direction of Profs. Ahmed Elgamal and Jose Restrepo.

References

- AISC. 2005. Specification for Structural Steel Buildings. Standard ANSI/AISC 360-05, American Institute of Steel Construction, Chicago, Ill., USA.
- ANSYS Multiphysics. 2007. ANSYS Element Reference. Release 11.0, Documentation for ANSYS. ANSYS Inc.
- ASCE. 2005. Minimum design loads for building and other structures. Standard ASCE/SEI 7-05. American Society of Civil Engineers, Reston, Va., USA.
- Atkinson, G.M. 2009. Earthquake time histories compatible with the 2005 *National Building code of Canada* uniform hazard spectrum. Canadian Journal of Civil Engineering, **36**(6): 991–1000. doi:10.1139/L09-044.
- Barros, R.C., and Almeida, R. 2005. Pushover analysis of asymmetric three-dimensional building frames. Journal of Civil Engineering and Management, **11**(1): 3–12.
- Bazeos, N., Hatzigeorgiou, G.D., Hondros, I.D., Karamaneas, H., Karabalis, D.L., and Beskos, D.E. 2002. Static, seismic and stability analyses of a prototype wind turbine steel tower. Engineering Structures, **24**(8): 1015–1025. doi:10.1016/S0141-0296(02)00021-4.
- CEN. 2005. Eurocode 3: Design of steel structures, Part 1.1: General rules and rules for buildings. Standard EN 1993-1-1:2005, European Committee for Standardisation, British Standards Institution, London, UK.
- CSA. 2001. Antennas, Towers, and Antenna-Supporting Structures. Standard CAN/CSA S37-01, Canadian Standards Association, Toronto, Ont.
- CSA. 2004. Steel (Fixed Offshore) Structures. Standard CAN/CSA S473-04. Canadian Standards Association, Toronto, Ont.
- CSA. 2008. Wind turbines – Part 1: Design requirements. Standard CAN/CSA C61400-1:08. Canadian Standards Association, Toronto, Ont.
- CSA. 2009. Design of steel structures. Standard CSA-S16-09. Canadian Standards Association, Toronto, Ont.
- Danish Wind Industry Association. 2003. Manufacturing wind turbine towers. [Online.] Available from <http://www.talentfactory.dk/en/tour/manu/towerm.htm> [accessed 8 April 2009].
- Deierlein, G.G., Liel, A.B., Haselton, C.B., and Kircher, C.A. 2008. ATC-63 methodology for evaluating seismic collapse safety of archetype buildings. ASCE-SEI Structures Congress, Vancouver, B.C., 24–26 April 2008.
- Elchalakani, M., Zhao, X.L., and Grzebieta, R. 2002. Bending tests to determine slenderness limits for cold-formed circular hollow sections. Journal of Constructional Steel Research, **58**(11): 1407–1430. doi:10.1016/S0143-974X(01)00106-7.
- IEC. 2005. Wind turbines – Part 1: Design requirements. 3rd ed. Standard IEC 61400-1:2005-08. International Electrotechnical Commission, Geneva, Switzerland.
- Lavassas, I., Nikolaidis, G., Zervas, P., Efthimiou, E., Doudoumis, I.N., and Baniotopoulos, C.C. 2003. Analysis and design of the prototype of a steel 1-MW wind turbine tower. Engineering Structures, **25**(8): 1097–1106. doi:10.1016/S0141-0296(03)00059-2.
- Nasserasadi, K., Ghafory-Ashtiani, M., Eshghi, S., and Zolfaghari, M.R. 2008. Developing seismic fragility function of structures by stochastic approach. Journal of Applied Sciences, **8**(6): 975–983. doi:10.3923/jas.2008.975.983.
- NBCC. 2005. National Building Code of Canada. National Research Council of Canada, Ottawa, Ont.
- Powell, I., Veletzos, M., Elgamal, A., and Restrepo, J. 2008. Shake table test of a 65 kW wind turbine and computational simulation. In 14th World Conference on Earthquake Engineering, Beijing, China, 12–17 October 2008, Paper ID 12-01-0178.
- Powell, I., Veletzos, M., Elgamal, A., and Restrepo, J. 2009. Experimental and Numerical Seismic Response of a 65 kW Wind Turbine. Journal of Earthquake Engineering, **13**(8): 1172–1190.
- Ritschel, U., Warnke, I., Kirchner, J., and Meussen, B. 2003. Wind turbines and earthquakes. In Proceedings of the 2nd World Wind Energy Conference (WWEC), Cape Town, South Africa, 24–26 November 2003.
- Somerville, P., Punyamurthula, S., and Sun, J. 1997. Development of ground motion time histories for Phase 2 of the FEMA/SAC Steel Project. Report No. SAC/BD-97/04, SAC Joint Venture, Sacramento, Calif., USA.
- Vamvatsikos, D., and Cornell, C.A. 2002. Incremental dynamic analysis. Earthquake Engineering & Structural Dynamics, **31**(3): 491–514. doi:10.1002/eqe.141.
- Voth, A.P. 2010. Branch plate-to-circular hollow structural section connections. Ph.D. thesis, Department of Civil Engineering, University of Toronto, Toronto, Ont.
- Witcher, D. 2005. Seismic analysis of wind turbines in the time domain. Wind Energy (Chichester, England), **8**(1): 81–91.
- Zhao, X., and Maisser, P. 2006. Seismic response analysis of wind turbine towers including soil-structure interaction. Proceedings of the Institution of Mechanical Engineers, Part K: Journal of Multi-body Dynamics, **220**(1): 53–61. doi:10.1243/146441905X73691.

List of Symbols

D	outside diameter of a CHS
DS	damage state
E	Young's modulus of elasticity
F_u	ultimate tensile stress
F_y	yield tensile stress
H	hub height of wind turbine tower
I	moment of inertia
IM	intensity measure
LP	load pattern
M	bending moment
M_p	plastic moment of a cross-section
M_y	yield moment of a cross-section
PGA	peak ground acceleration
t	thickness
T_i	period of mode i
α_i	modal participation factor of mode i
Δ	lateral deflection
Δ_{\max}	peak lateral displacement
Δ_{res}	residual lateral displacement
ε_u	ultimate strain at fracture
θ_{\max}	maximum rotation of tower as defined in this paper
κ	curvature
κ_p	curvature at plastic moment: M_p/EI
μ	average or mean, used in defining fragility curves
σ_{mises}	von Mises stress
ϕ_i	mode shape of mode i , normalized to mass matrix